


# Experimental analyses of synthetic jet control effects on aerodynamic characteristics of helicopter rotor

Y.Y. Ma,  Q.J. Zhao, X. Chen and G.Q. Zhao  
[zhaoqijun@nuaa.edu.cn](mailto:zhaoqijun@nuaa.edu.cn)

National Key Laboratory of Science and Technology on Rotorcraft Aeromechanics  
Nanjing University of Aeronautics and Astronautics  
Nanjing, 210016  
China

## ABSTRACT

Experimental analyses of synthetic jet control (SJC) effects on aerodynamic characteristics of rotor in steady state and in hover were conducted. To ensure the structural strength of rotor and enough interior space for holding the synthetic jet actuators (SJAs), a particular blade with a frame-covering structure was designed and processed, and the experiment was conducted with low free stream velocities and rotor rotation speeds. There were three test conditions. In steady state, there were three free stream velocities (10m/s, 15m/s and 20m/s). In hover state, the rotor was worked with two rotation speeds of 180RPM and 240RPM. In forward flight, the rotor was worked with a rotation speed of 180RPM and a free stream velocity of 7.5m/s. To measure the synthetic jet control effect on rotor in stall, the range of collective pitch was set from 10° to 28° in steady state. The aerodynamic forces and sectional velocity field were measured by using the six-component balance and the Particle Image Velocimetry (PIV) system in the wind tunnel. Flow control effects on the blade based on the synthetic jets (SJ) were experimentally investigated with different jet parameters, such as jet locations, jet angles, and jet velocities. In steady state, the jet closer to the leading edge, and the jet angle of 90° had more advantages in improving the aerodynamic characteristics. Furthermore, the aerodynamic forces and sectional velocity field measurement of rotor in hover were conducted, it showed that SJAs could increase flow velocity at the upper surface, which led to lower upper surface pressure. As a result, the normal forces of rotor with two rotation speeds were increased significantly. These results indicated that the synthetic jet has a capability of increasing the normal force and delaying or preventing the stall of rotor.

**Keywords:** Synthetic jet; Blade; Rotor; Flow separation; Wind tunnel; Particle Image Velocimetry; Experiment

## NOMENCLATURE

$c$	=	chord
$F$	=	excitation frequency
$R$	=	radius of rotor
$U_{\text{jet}}$	=	excitation voltage
$\alpha$	=	angle of pitch
$F_y$	=	normal force of rotor
$\theta_{\text{jet}}$	=	synthetic jet angle

## 1.0 INTRODUCTION

Due to a combination of freestream velocity and rotation velocity of rotor, helicopter rotor encounters different flow conditions at advancing (transonic) and retreating (low-speed) sides respectively<sup>(1)</sup>. These phenomena may induce large negative pitching moments which might bring on excessive vibration load and flutter of rotor, and further limits the operational envelope of helicopter<sup>(2)</sup>.

In recent years, concepts such as fixed and dynamic slats, variable droop leading-edge airfoils (VDLEs), synthetic jet control, and trailing-edge flaps (TEFs) have been considered for promising active flow control strategies of the advanced rotor in the future<sup>(3)</sup>. Of these, SJC appears attractive since its control system is expected to be a compact, low-actuation-power, and high-bandwidth device that can be used for multifunctional roles such as vibration and noise suppression and rotor performance enhancement.

As a novel active flow control method, many investigations about the synthetic jet control for improving aerodynamic characteristics have been conducted<sup>(4–7)</sup>. Seifert conducted active control experiments on NACA0015 airfoil<sup>(8,9)</sup>, and the capability of the synthetic jet on delaying the stall of the airfoil was verified. Gilarranz conducted the experimental investigations about the effects of a synthetic jet actuator (SJA) on the aerodynamic performance of the wing<sup>(10,11)</sup>, and it indicated that the SJAs extend the stall angle of attack. Lee experimentally investigated the separation control by jet arrays for an inclined flat plate<sup>(12)</sup>. Amitay experimentally investigated the control effects of SJAs on the flow separation of an unconventional symmetric airfoil<sup>(13)</sup>. Based on numerical simulation method developed by CLORNS code<sup>(14)</sup>, Zhao conducted parametric analyses for an OA213 airfoil to investigate the synthetic jet control effects on the dynamic stall characteristics of the airfoil<sup>(15)</sup>. These works all indicated that the synthetic jet is an efficient technology to control the flow separation and the stall of the airfoil<sup>(15–18)</sup>, and it may be a benefit for preventing dynamic stall of rotors<sup>(15)</sup>.

Due to the difficulties of the installing of SJAs in the blade and the complexity of rotor motion, the synthetic jet control effect on the aerodynamics of rotors were mainly conducted using the numerical simulation methods by now. Hassan simulated the effects of surface bowing and suction on the aerodynamic characteristics of the MD-900 rotor by solving the unsteady 3D full-potential equations<sup>(19)</sup>. Dindar numerically investigated the potential merits of using the flow control on rotor in hovering flight<sup>(20)</sup>. Although some meaningful results are obtained through these numerical works<sup>(19–21)</sup>, few experimental investigations on the application of synthetic jet on rotors are found in the public domain<sup>(22)</sup>, resulting in the lack of the corresponding validations for numerical investigations of SJC on rotors. As a result, the

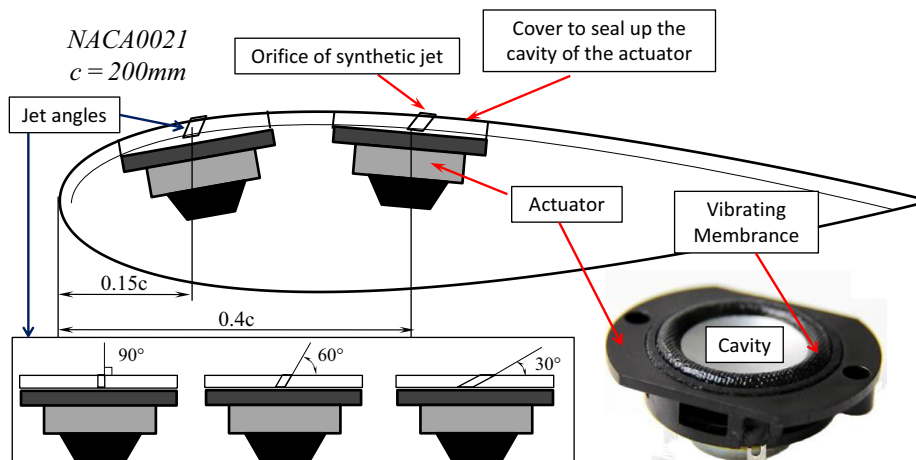


Figure 1. The installation of synthetic jet actuators in the model.

investigations of the synthetic jet on rotor are still theoretic at present. Additionally, there are still some problems which have not been overcome in the applications of synthetic jets on airfoil<sup>(23)</sup>, such as the choice of the jet parameters<sup>(24,25)</sup>.

Based above, the purpose of this paper was to conduct a principle experimental investigation for the synthetic jet control effects on the blade in steady state and rotor in hover. For the application of SJAs in the blade, a particular blade with a frame-covering structure was designed and processed. The surface pressures of the section were measured by piezometric tube. The aerodynamic forces and the sectional velocity field of the blade were measured by the six-component balance and the Particle Image Velocimetry (PIV) system, respectively. Through the comparisons of test results with and without the SJC, the synthetic jet had a capability of improving the blade aerodynamic characteristics when the dynamic stall occurred, and it may have better control effects on increasing normal forces of rotor in hover, because the SJAs could increase flow velocity at the upper surface, which led lower upper surface pressures. The control effects of the synthetic jet were also investigated with different jet parameters, such as jet locations, jet angles, and jet velocities, and some new control laws were obtained.

## 2.0 EXPERIMENTAL PLATFORM AND PROCEDURE

### 2.1 Blade model and synthetic jet array

Considering the size of the synthetic jet actuators (SJA) and the installation of the actuator arrays in the blade model, the blade using NACA0021 airfoil was used as test model with a chord of 0.2m and a span 1m. Based on the previous investigations<sup>(25)</sup>, the one-inch full range speaker units were used as the jet actuators, and three inclined angles of the synthetic jet movement were achieved by using different covers with varied outlet angles (30°, 60°, and 90°). The illustration of the SJA and its placement in the model is shown in Fig. 1.

The parameters of experimental blade model and jet actuators are shown in Table 1. It is suggested that flow separation occurs at 15%*c* by numerical simulation<sup>(15)</sup> and test of the airfoil stall<sup>(25)</sup>. So the SJA were positioned at 15%*c* and 40%*c* respectively, and there were

**Table 1**  
**Parameters of blade model and jet actuators**

Parameter	Value
Airfoil	NACA0021
Chord $\times$ span (mm)	200 $\times$ 1200
Width $\times$ length of jet orifice (mm)	1.5 $\times$ 20
Jet angle ( $^{\circ}$ )	30, 60, 90
Chordwise location(c)	15%, 40%
Spanwise location(R)	55% ~ 85%
Spanwise interval(R)	5%
Size of jet actuator (mm)	40 $\times$ 33 $\times$ 14
Resistance of actuator ( $\Omega$ )	8

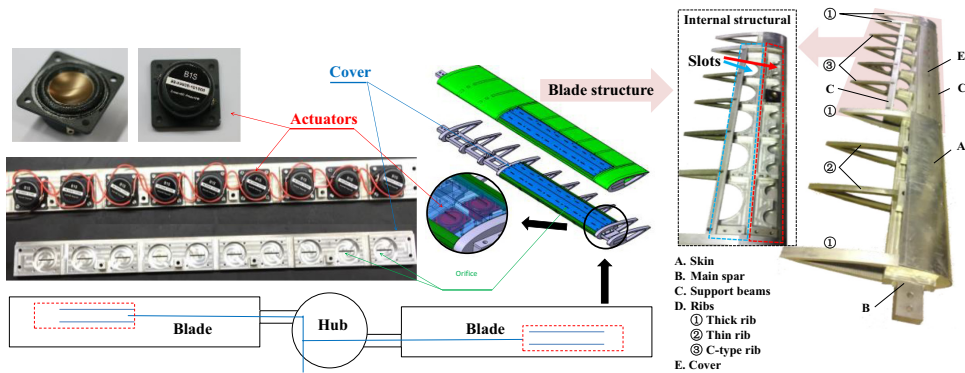


Figure 2. The installation of SJAs and the structure of the blade.

9 SJAs at the spanwise direction with the length of the orifice being 20mm and the spacing 40mm.

To ensure the structural strength of the blade and the enough interior room for installing the actuators, a frame-covering structure was applied in the process of the particular blade, as shown in Fig. 2. The frame consisted of a main spar, several ribs (the thick rib, the thin rib and the c-type rib) and two support beams for the covers. All the ribs were hollowed to decrease the weight and to move the center of gravity forward. Two electronic circuits were fixed in the range from the blade root to the 0.5R section, and the electrical signals could be transmitted from the functional signal generator on the ground to the actuators on the covers through the collective ring. The covers were fixed on the blade by the screws, and they were removable. On the lower surface of the covers, there are several circular grooves to apply the cavity for the generation of the synthetic jet. The nine actuators were firmly fixed on the surface of the cover, and the air-tightness between them was guaranteed by the sealing, and the nine actuators were connected with each other in a parallel circuit. The connectors between the circuits on the covers and those on the main spar were pluggable. Thus it was possible to change conveniently the covers with different jet angles on the blade in the experiment.

Figure 3 shows that the root mean square (RMS) velocity varies with the excitation frequency  $F$  at the centerline of jet orifice of an isolated actuator according to different

**Table 2**  
**Correspondence between the voltage and velocity**

Excitation voltage (V)	Jet mean velocity (m/s)
3	9.8
4	12.2
5	14.4

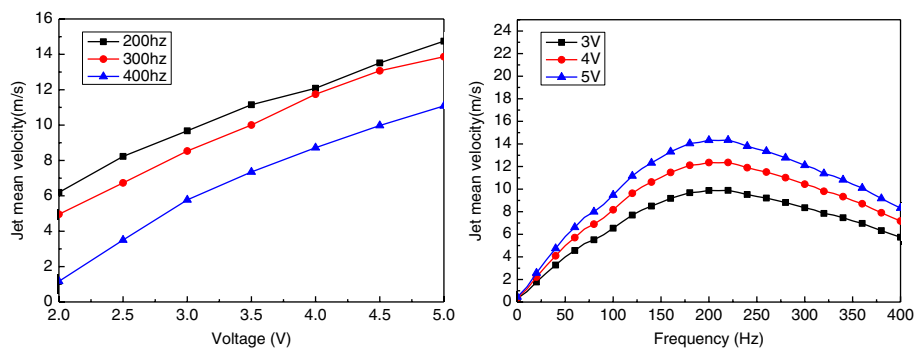


Figure 3. Velocity of jet actuator with respect to relative excitation frequency and voltage.

excitation voltages. The estimate of measurement uncertainty for the velocity is about 1.5%. As shown in the figure, the RMS velocity of jet increases with a larger excitation voltage  $U_{jet}$ , and there is a peak RMS velocity when the excitation frequency is about 200Hz. So the excitation voltage of SJA was set up to 5V with a fixed excitation frequency being 200Hz, which was adopted in the whole test. Since the excitation voltage and jet velocity are almost linear, so the excitation voltage were used to present the strength of the synthetic jets. Table 2 gives the correspondence between the voltage and velocity.

### 2.2 Measuring equipment

The principle experimental tests for synthetic jet control effect were conducted in a low-speed return flow wind-tunnel (with a rectangle experimental section about 3.2m × 2.4m) of Nanjing University of Aeronautics and Astronautics. The experiments included the aerodynamic force measurements and the sectional velocity field measurements. The measurement system for the aerodynamic force of model rotor under the control of SJAs included the six-component balance, the functional signal generator, the signal amplifier, the 16-bit data acquisition card, the computers, and the special testing software. The PIV system for the sectional velocity field measurements contained the double pulse laser source, the optical element, the CCD camera, the synchronizing device, the insight 3G processing programs, and the traditional trace particle generators. Table 3 gives the main parameters of PIV system, and Fig. 4 shows the PIV measuring scene.

### 2.3 Experimental content and method

Due to the difficulty of the special rotor model processing, the present blade was much heavier with a weight of about 4kg. For security considerations, principle experiments for synthetic

**Table 3**  
**Main parameters of PIV system**

Parameters	Value
Single pulse width (ns)	<10
Pulse duration (ms)	0.5
pulse Frequency (Hz)	1.6–3.2
The resolution of CCD camera (Pixel)	1066 × 1208
Time interval of two frames (us)	<1
Valid measure-zone(mm)	400 × 400

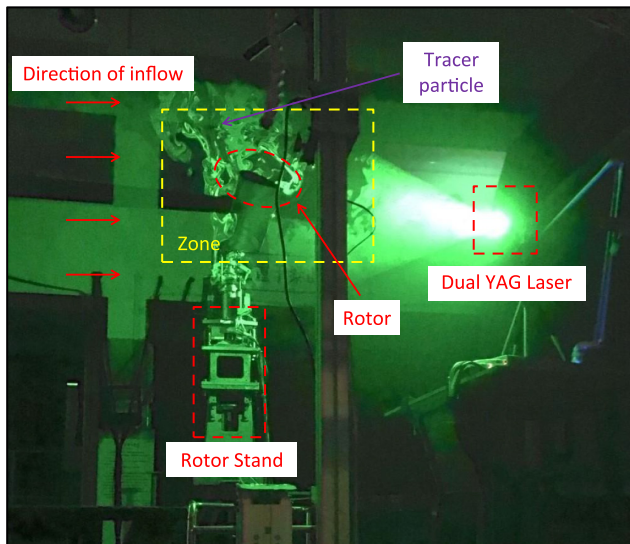


Figure 4. PIV measuring scene.

jet control effects on rotor in steady state and in hover were conducted with low rotor rotation speeds (180RPM and 240RPM) and low free stream velocities (10m/s, 15m/s and 20m/s). The measurements were carried out at  $Re \approx 0.7 \times 10^5 \sim 3.5 \times 10^5$  in a flow having a free-stream turbulence intensity of about 1.2% by the hot wire anemometer. The blade model was mounted on a shrouded six-component force and moment balance located in the rotor stand.  $F_y$  was the force perpendicular to the plane of rotation obtained from the balance whose sampling rate is 50Hz and uncertainty of force is 3%. Also,  $F_y$  was unsteady data and an average over three seconds. The angle of pitch was relative to the plane of rotation and adjustable through a range of  $14^\circ < \alpha < 28^\circ$ , using a computer-controlled actuator. The excitation voltage of jet actuator was ranging from 3 to 5V (0V is the baseline case without jet control). In order to capture the detail information of local flowfield over blade section, the 0.8R sectional velocity field at  $270^\circ$  azimuthal angle was measured by PIV system. There were 200 images used for averaging and the valid measure-zone was located over the upper surface of  $r = 0.8R$  section of blade. When the rotor is rotating, the flowfield was measured by PIV system with a phase locking technique. The imported signal was originated from the function signal generator on

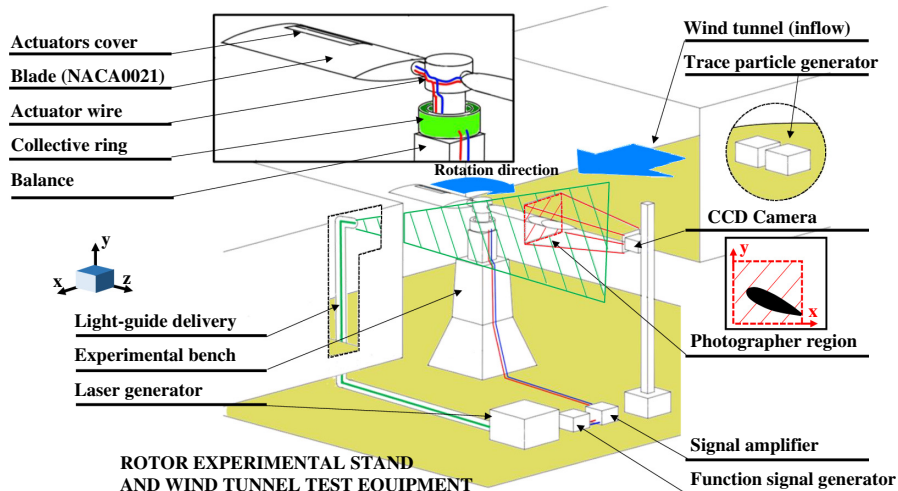


Figure 5. Schematic figure of experiment and PIV measurement zone.

the ground, and it was transmitted to the SJAs by the collective ring during the rotor rotation. Figure 5 shows the schematics of the measurements of model aerodynamic force and PIV measurement zone. In the steady state experiment, the synthetic jets are actuated on one blade and the backwards facing blade is removed. The root of blade is fixed on the hub, but the tip of blade can flap with the normal force changes. In hover and forward flight, the synthetic jets are actuated on both blades and they could rotate.

## 3.0 RESULTS AND DISCUSSIONS OF SYNTHETIC JET CONTROL EFFECTS OF BLADE IN STEADY STATE

### 3.1 Control effects of blade over stall

Firstly, the control effects of synthetic jet on preventing flow separation at large AoA were investigated, and Fig. 6 illustrates the speed contours and streamline diagram over the upper surface of  $r = 0.8R$  section w/o jet control at  $\alpha = 19^\circ$  with 15m/s inflow and  $\alpha = 17^\circ$  with 10m/s inflow. In the both inflow conditions, the SJAs at 15%c of the blade were turned on with a jet angle of  $90^\circ$  and an excitation voltage of 5V.

As it can be seen, the stall vortex forms at leading edge and its convection along the upper surface of  $r = 0.8R$  section induces the large flow separation, which leads to the large-scale recirculation region near the trailing edge. The large flow separation finally causes the loss of lift of blade, which threatens the performance of rotor. With control of synthetic jet near the leading edge, the mixing between the internal and external layer of the flow in the boundary layer is heightened, the energy of the boundary layer is strengthened at the same time. Both the two effects could lead to the effective inhibition of the leading-edge vortex, and further make the separation point move downstream along the upper surface, thus it could significantly reduce the large flow separation region as shown in the figure.

To verify the control effects of synthetic jet on normal force  $F_y$  and stall of blade, the jet control tests were conducted with the Actuators 1 (A1) at 15%c of profile airfoil turned on under two different free stream velocities (15m/s and 20m/s). Figure 7 shows a comparison of



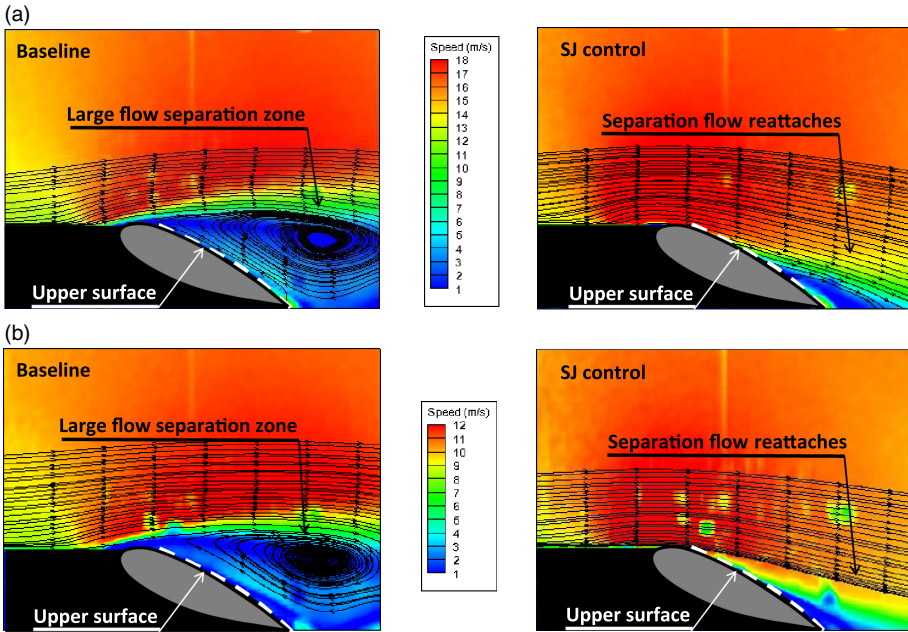


Figure 6. Speed contours and streamline diagram under synthetic jet control. (a)  $\alpha = 19^\circ$  with 15m/s inflow A1 ( $5V, 90^\circ$ ) was turned on. (b)  $\alpha = 17^\circ$  with 10m/s inflow A1 ( $5V, 90^\circ$ ) was turned on.

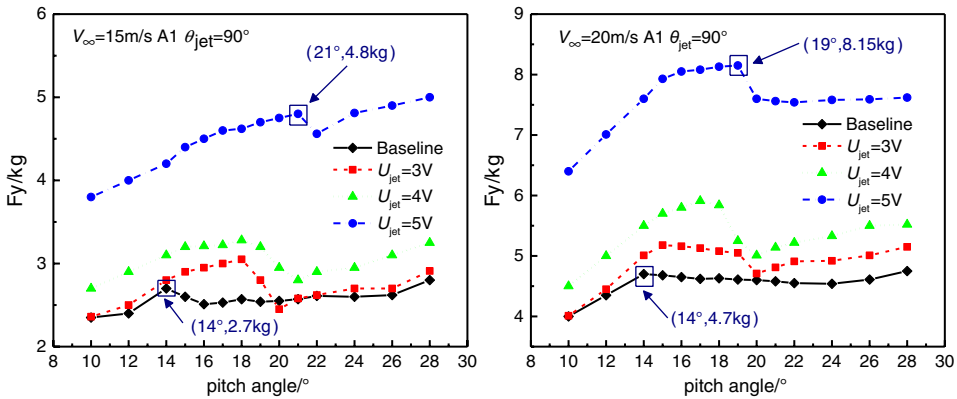


Figure 7. Comparison of the variation of normal forces under different excitation voltages.

the normal forces under different excitation voltages  $U_{jet}$  with  $90^\circ$  jet angle. As shown in the figure, there are discontinuities when the stall occurs with maximum normal force. Under the control of synthetic jet, the normal force and stall angle of blade both increase significantly. Additionally, as the excitation voltage increases, the control effects on improving the aerodynamic characteristics of blade become better. Under two different free stream velocities, there are about 2.1kg and 3.45kg increment of the maximum normal force of blade and about 7 degrees and 5 degrees angle of attack delay of stall respectively at 5V voltage compared to the baseline case.



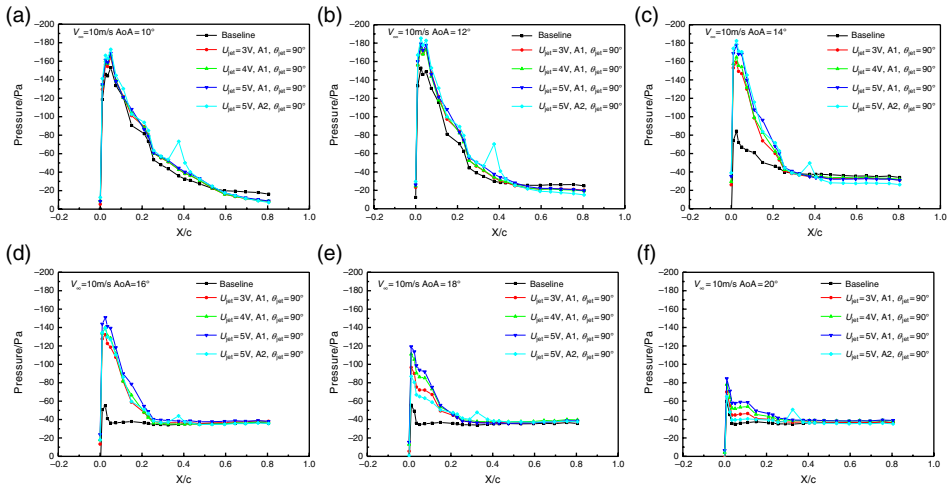


Figure 8. Upper surface pressures of the controlled section with 10m/s inflow. (a) 10°. (b) 12°. (c) 14°. (d) 16°. (e) 18°. (f) 20°.

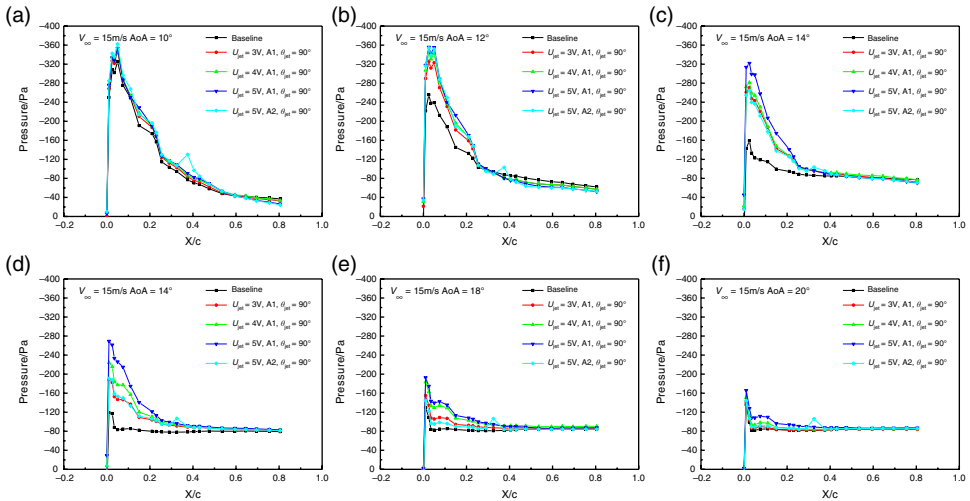


Figure 9. Upper surface pressures of the controlled section with 15m/s inflow. (a) 10°. (b) 12°. (c) 14°. (d) 16°. (e) 18°. (f) 20°.

By measurements of surface pressure distributions of  $r = 0.8R$  section of a controlled blade with 23 piezometric tubes, the control effects of synthetic jet on aerodynamic force of a controlled blade were investigated. The pressure data were obtained when the motion of the blade is steady and the uncertainty for pressure is 1.5%. Figures 8 and 9 shows the results of the surface pressure measurements with different excitation voltages and locations, and the jet angle is always 90°. The two different free stream velocities are 10m/s and 15m/s and the angles of attack is various ranging from 10° to 24°. As it can be seen, when jet control is turned on, the upper surface pressures of the controlled section are significantly decreased.

**Table 4**  
**Ratios of jet mean velocities to free stream velocities**

Ratios	Free stream velocity (m/s)			
	10	15	20	
	9.8	0.98	0.65	0.49
Jet mean velocity (m/s)	12.2	1.22	0.81	0.61
	14.4	1.44	0.96	0.72

When the angle of attack is small (Figs. 8 (a) and 9(a)), no flow separation occurs on the surface of the airfoil, so the control effect of the jet is not obvious and the jet with different velocities has little effect on the upper surface pressure.

As the angle of attack increases (Figs. 8(b)-(d) and 9(b)-(d)), flow separates at the leading edge, and the upper surface pressures of the controlled section are significantly lower than the previous ones. Also, the larger jet velocity has a more obvious effect in reducing upper surface pressures. This is mainly due to the reason that with the RMS velocity increases, the interaction between synthetic jet and separated flow becomes more intense, and the mixing influence of the jet is more effective, with which can better increase flow velocity at the upper surface, and further lead to the increment of the lift. Also, the blue line is always above the cyan line, which means the lower surface pressure (Figs. 8(b)-(d) and 9(b)-(d)), so the effect of lift-enhancement via synthetic jet at 15% $c$  is more obvious than at 40% $c$ .

As the angle of attack is further increased (Figs. 8(f) and 9(f)), the upper surface of the controlled airfoil is also separated. At this time, the differences with and without synthetic jet control become small. It is necessary to point out that there is a sudden drop of surface pressure at 40% $c$  when the synthetic jet at 40% $c$  is turned on. Furthermore, as the magnitude of the inflow increased, the control effects of jet become mitigated.

### 3.2 Effects of jet velocity

The RMS velocity is an important parameter of synthetic jet, to investigate its influences on the control effects on blade stall and flow separation, three excitation voltages (3~5V, with respecting jet velocity about 9~15m/s) were conducted to explore the effects of velocity of synthetic jet on enhancing the aerodynamic characteristics of a stalled blade. Table 4 gives the different ratios of jet mean velocities to free stream velocities.

Figure 10 shows the normal force of blade under control of different combinations of actuators with two free stream velocities and different pitch angles. At the inflow condition with fixed freestream velocity, the increase of jet excitation voltage leads to the increase of jet momentum coefficient. As a result, the control effects of synthetic jet on the maximum normal force of blade are enhanced with the jet velocities increases.

It is obvious that a jet with a larger velocity could enhance the interactions between the periodic synthetic jet and the flow in boundary layer, and it could also enhance the mixing of the inner and outer layer of the boundary layer resulting in the stability of the shear layer and the larger stall incidence.

Though the SJ could significantly improve the aerodynamic characteristics of blade at large pitch angle of blade without stall, the enhancement of the normal force of blade may be reduced at larger AoA in stall. It is because that the separation point moved toward the leading-edge as AoA increases, and the jet in the recirculation zone with small velocity has not enough energy to control the large flow separation.

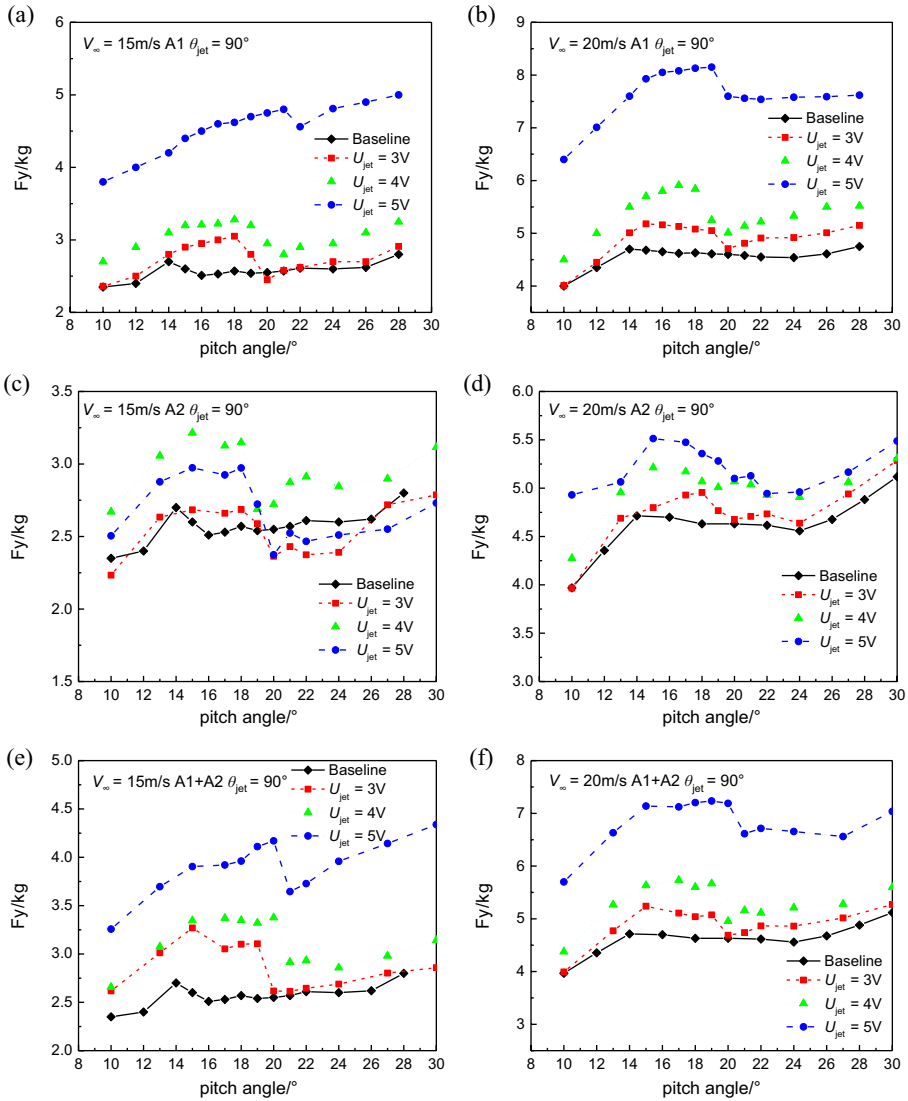


Figure 10. Control effect of SJAs with different jet velocities on the normal force of blade. (a) A1(15%c), 15m/s,  $90^\circ$ . (b) A1(15%c), 20m/s,  $90^\circ$ . (c) A2(40%c), 15m/s,  $90^\circ$ . (d) A2(40%c), 20m/s,  $90^\circ$ . (e) A1(15%c) +A2(40%c), 15m/s,  $90^\circ$ . (f) A1(15%c)+A2(40%c), 20m/s,  $90^\circ$ .

### 3.3 Effects of synthetic jet location

The investigations of control mechanism according to different locations of SJA were carried out by comparing the different control effects of two SJAs located at different chordwise positions. Actuators 1 (A1) were placed at 15%c on the suction upper surface of profile airfoil while the other ones (A2) were at 40%c on the upper surface.

Figure 11 shows the comparisons for the control effects of the synthetic jet under different inflow conditions with varied momentum coefficients and locations. Obviously, the

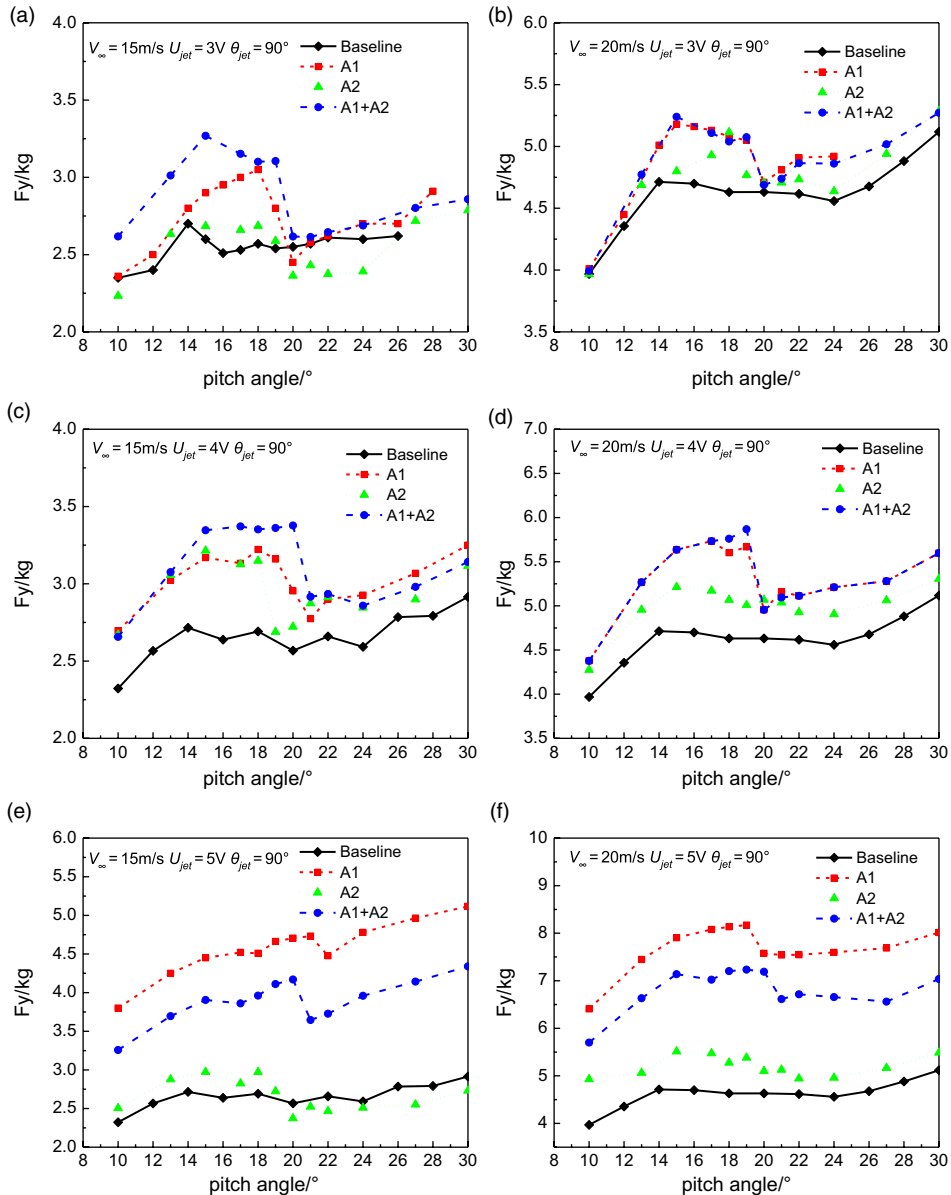


Figure 11. Control effect of SJAs with different jet locations on the normal force of blade. (a) 3V, 15m/s, 90°. (b) 3V, 20m/s, 90°. (c) 4V, 15m/s, 90°. (d) 4V, 20m/s, 90°. (e) 5V, 15m/s, 90°. (f) 5V, 20m/s, 90°.

performance of A1 on delaying stall of airfoil is more outstanding than A2. It is because that the loss of lift in stall was induced by the large flow separation at the leading-edge, and A1 is nearby the separation point and the starting position of the shear layer, so the periodic jet formed at the orifice of A1 could directly energize the boundary layer and enhance the mixing of the shear layer. The intensive interactions induced by the SJA help to further delay the stall of airfoil. Moreover, the A2 with a 90° jet angle may antedate the stall of blade.

Compared with unique jet actuator, the dual-jet could lead to a more significant increment of normal force of blade, when the magnitude of jet velocity is relatively small. With the increase of the jet velocity, the gaps among the control effects due to A1 and the dual-jet become narrow. When  $U_{\text{jet}}$  is 5V, the control effects of A1 on stall of blade are better than those of dual-jet.

### 3.4 Effects of jet array at different jet angles

The jet angle is an important parameter of synthetic jet, it is necessary to find out the reasons for further investigations of the mechanism of jet control on delaying stall of blade. In this paper, two inflow conditions (15 and 20m/s) were conducted to carry out the experimental-parametric analyses. Figure 12 shows the increasing rates of max normal force increments of airfoil stall angles under control of A1, A2 and both with different jet angles at two inflow conditions.

As shown in the figure, when the inflow velocity is 15m/s, the max normal force before stall may be reduced under the control of A1 with small jet angle, but the stall angle is still improved due to the energy injection of the jet. It indicates that if the jet velocity is too small to control the flow separation, the control effect of SJAs will be a negative for the aerodynamic characteristics of the rotor. The control effects of the A1 become obvious as jet angle increasing. When the angle becomes larger, the synthetic jet will actually act more like a vortex generator which is effective in delaying the separation and the normal jet could energize the main flow more intensively and directly, and then it could enhance the stability of the boundary layer more efficiently.

The difference between the control effects of the A2 with different jet angles is not significant, the control effect is slightly better when jet angle is 60°. Compared with unique jet actuator, the influence of the dual-jet is not much affected by the jet angle, since the energy supplied by two SJAs is sufficient. As the magnitude of the inflow increases (20m/s for example), the control effects become more significant and the gaps among them due to jet angle on increasing the normal force of blade and stall angles are narrowed. These phenomena are similar to the numerical results of He<sup>(24)</sup>.

Overall, the control mechanisms of SJA on improving aerodynamic characteristics of blade affected by the jet angle are a little different at different free stream velocities. The interactions induced by synthetic jet to the flowfield over airfoil are mainly attributed to the mixing effects, and a jet with a larger inclined angle could enhance the mixing effects between the inner and outer layer of boundary layer.

The experimental results indicate that the influences of jet angle to the stall control of airfoil using synthetic jet are very complicated, and a jet with a specific jet angle could not obtain the best control effects in all the inflow conditions, and the jet angle's effects may be also depended on the jet momentum coefficient. Better control effects could be obtained by the control of a jet with a larger jet angle when the jet momentum coefficient is small to a certain extent.

## 4.0 RESULTS AND DISCUSSIONS OF SYNTHETIC JET CONTROL EFFECTS OF ROTOR IN HOVER

### 4.1 Control effects of rotor in hover

To investigate the synthetic jet control effects on rotor in hover, the aerodynamic force measures for rotor and the sectional velocity field measure were conducted. In this test, the SJAs

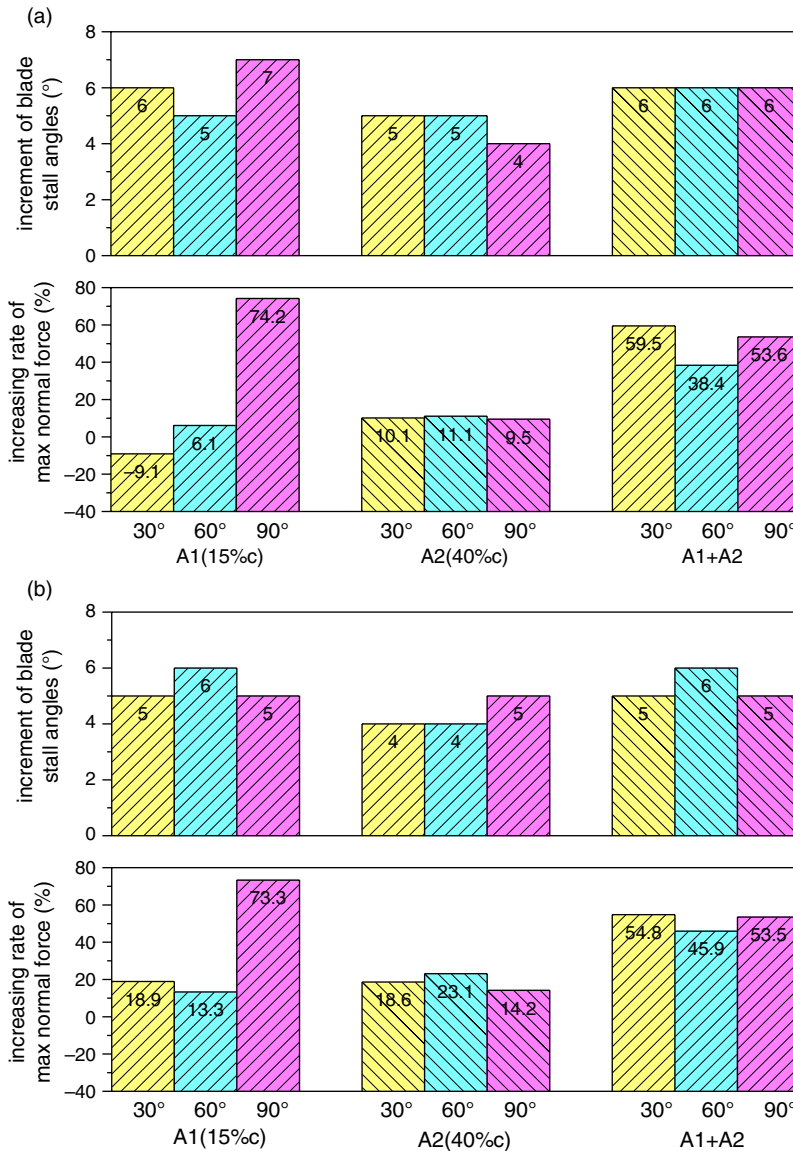


Figure 12. Control effect of SJAs with different parameters on the normal force and stall angle of blade. (a) 5V, 15m/s. (b) 5V, 20m/s.

at 15%c of the blade were turned on with a jet angle of 90° and an excitation voltage of 5V, and the rotor was worked with two rotation speeds of 180RPM and 240RPM. Table 5 gives the different ratios of jet mean velocities to tip speeds and Table 6 gives the ratios of jet frequencies to the angular velocities of rotor.

Figure 13 shows  $F_y$  of the rotor with and without SJC. As seen,  $F_y$  increase significantly with two rotation speeds, which are similar to that in the steady state, and it indicates that the SJC has a capability of improving the aerodynamic characteristic of rotor in hover.

**Table 5**  
Ratios of jet mean velocities to tip speeds

Ratios	Tip speeds (m/s)		
	22.62 (180RPM)	30.16 (240RPM)	
Jet mean velocity (m/s)	9.8	0.43	0.32
	12.2	0.54	0.40
	14.4	0.64	0.48

**Table 6**  
Ratios of jet frequencies to angular velocities of rotor

Ratios	Angular velocity of rotor (Hz)		
	3 (180RPM)	4 (240RPM)	
jet frequency (Hz)	200	66.7	50

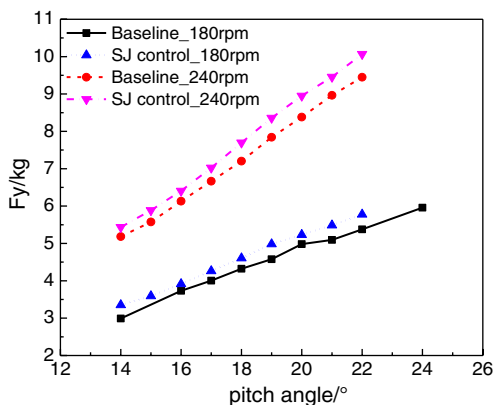


Figure 13. Control effect of SJAs on the normal force of rotor in hover with two rotation speeds.

Through the PIV technology and the phase lock technique, Figure 14 shows the sectional speed at 90° azimuthal angle with and without SJC at a pitch angle of 20°, a rotation speed of 180RPM. The streamlines and contours of speed are decided by the relative velocity ( $U_{ref}$ ) to the blade. As seen, there is a larger high-speed region at the upper surface due to the control of SJAs, which keeps consistent with section 3.1. It means the SJAs could increase flow velocity at the upper surface. Therefore, the lift of rotor has been improved in hover.

### 4.2 Effects of jet velocity and jet angle

The influences of jet velocity and jet angle on aerodynamic characteristics of the rotor in hover were conducted. Firstly, the SJAs at 15% of the blade were turned on with a jet angle of 90° and three different excitation voltages (3~5V, with respecting jet velocity about 9~15m/s). Figure 15 shows the  $F_y$  of the rotor with the rotation speed of 180RPM. As a result, synthetic



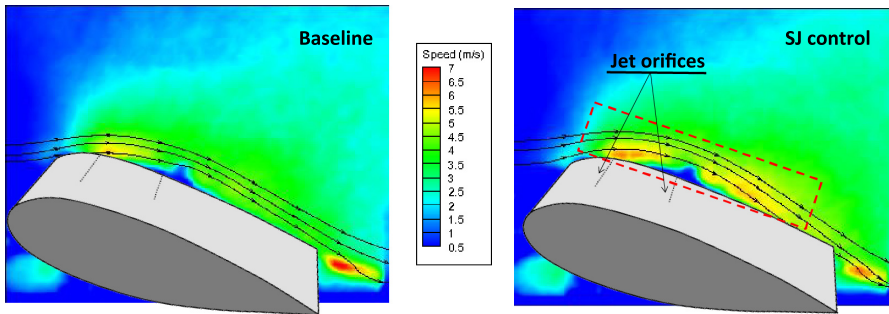


Figure 14. Comparisons of sectional speed contour and streamline diagram of the 0.8R blade section with and without the control of A1 (180RPM, 5V, 20m/s, 90°).

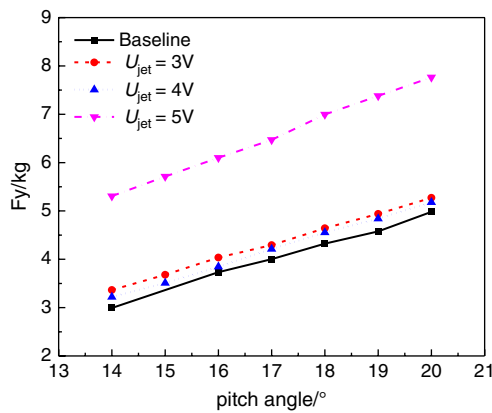


Fig. 15. Control effect of SJA with three different excitation voltages on the normal force of rotor in hover with the rotation speed of 180RPM.

jet with larger velocity has better control effects on the normal force of rotor, which re similar to them of blade in steady state.

Then, the SJAs at 15%c of the blade were turned on with excitation voltage of 5V and three different jet angles (30°, 60°, and 90°). Figure 16 shows the  $F_y$  of the rotor with the rotation speed of 180RPM. As it can be seen, A1 (90° and 30°) had a better control effect on the normal force.

## 5.0 RESULTS AND DISCUSSIONS OF SYNTHETIC JET CONTROL EFFECTS OF ROTOR IN FORWARD FLIGHT

To investigate the synthetic jet control effects on the rotor in forward flight, the aerodynamic force measures for the rotor and the sectional velocity field measure were conducted. In this test, the SJAs at 15%c of the blade were turned on with a jet angle of 90° and an excitation voltage of 5V, and the rotor was worked with a free stream velocity of 7.5m/s. So the advance ratio is 0.33.

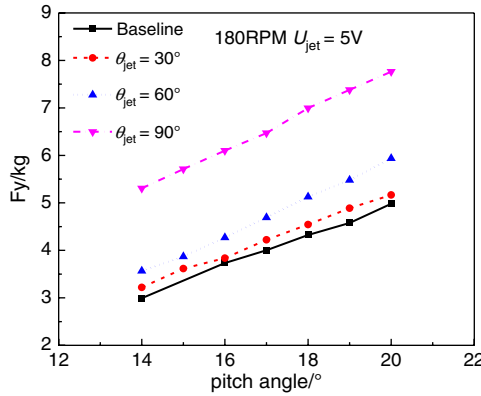


Figure 16. Control effect of SJA with three different jet angles on the normal force of rotor in hover with the rotation speed of 180RPM.

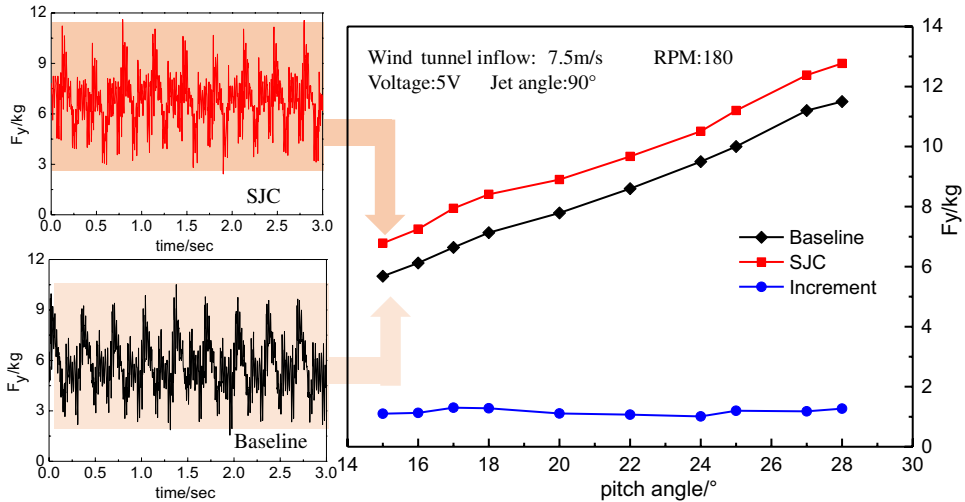


Figure 17. Control effects of SJAs on the normal force of the rotor in forward flight.

Figure 17 shows the  $F_y$  of the rotor in forward flight at different collective pitches with and without SJC. As it can be seen,  $F_y$  increased significantly similar to that in the steady state, and it indicated that the SJC has a capability of improving the aerodynamic characteristics of the rotor in forward flight.

Through the PIV technology and the phase lock technique, Figure 18 shows the sectional horizontal velocity ( $U$ ) at  $270^\circ$  azimuthal angle with and without SJC at a  $\theta_{jet}$  of  $15^\circ$ , a rotation speed of 180RPM and a free stream velocity of 7.5m/s. The stream line was decided by the relative velocity ( $U_{ref}$ ) to the blade and the vertical velocity ( $V$ ). As it can be seen, there was a large flow separation at the upper surface due to the large local angle of attack. Figure 19 shows the relative velocity ( $U_{ref}$ ) under the control of SJAs. There was still a flow separation on the upper surface, but the area of the flow separation region decreased significantly.

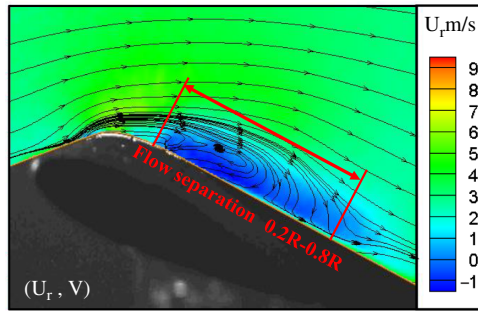


Figure 18. Horizontal velocity contours and streamline diagram of the 0.8R blade section at the 270° azimuthal angle without SJC ( $\theta_{\text{jet}} = 15^\circ$ ).

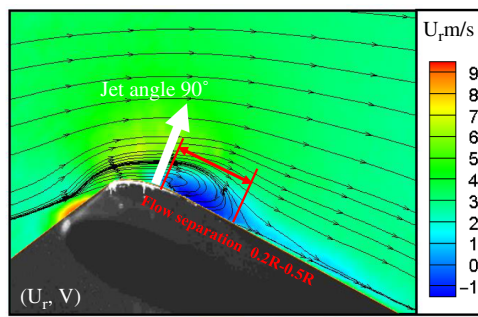


Figure 19. Relative velocity contours and streamline diagram of the 0.8R blade section at the 270° azimuthal angle with SJC ( $\theta_{\text{jet}} = 15^\circ$ ).

It means the SJAs could ease the flow separation phenomenon in the retreating blade and improve the aerodynamic characteristics of the rotor in forward flight.

## 6.0 CONCLUSIONS

In this paper, the principle experimental investigations for the synthetic jet control effects on the aerodynamic characteristics of the blade in steady state and rotor in hover were conducted. In the tests, the aerodynamic forces and the sectional velocity field of the blade were measured by the six-component balance embedded in the rotor platform and the PIV system respectively. The specific conclusions are shown as follows:

- (1) The control effects of the synthetic jet on the aerodynamic characteristic of rotor in steady state and in hover could be effectively investigated by the combination of the aerodynamic force measurements, the flow velocity measurements, and the surface pressure measurements. The SJAs applied on the blade have the capability in improving aerodynamic characteristics of rotor, especially in increasing the lift of rotor.
- (2) A synthetic jet with larger excitation voltages has better control effects on improving the aerodynamic characteristic of rotor. Additionally, if the excitation voltage of SJA near the middle along the chordwise direction is large, the aerodynamic characteristic of blade may get worse.

- (3) For the rotor in steady state, the SJAs near the leading edge (A1, 15%*c*) could enhance the aerodynamic characteristics more effectively compared with SJAs near the middle along the chordwise direction (A2, 40%*c*). Additionally, the dual-jet could lead to more significant increment of normal force of blade, compared to unique jet actuator
- (4) The SJAs near the leading edge with a jet angle of 90° might have a better control effect on the normal force and stall angle, while the SJAs with a jet angle of 30° might reduce the normal force of blade. And it is not obvious for the difference between the control effects of the SJAs near the middle along the chordwise direction with different jet angles.
- (5) For the rotor in hover, the SJAs could increase flow velocity at the upper surface, which leads lower upper surface pressures. Therefore, the lift of rotor is increased. For the rotor in forward flight, the flow separation region could be decreased significantly. If implemented in higher forward flight or higher rotation speed, the synthetic jet will need a larger excitation voltage to achieve the similar control effects.

In the next research work, high-efficiency synthetic jet actuators (a higher jet RMS velocity, a controllable jet angle and a smaller size) and a new special blade with a less weight will be developed and processed, and a systematic experimental investigation for synthetic jet control effect on rotor will be conducted.

## REFERENCES

1. CONLISK, A.T., Modern helicopter rotor aerodynamics. *Progress in Aerospace Sciences*, 2002, **37**, (5), pp 417–476.
2. YU, Y.H., LEE, S., MCALISTER, K.W., TUNG, C. and WANG, C.M. Dynamic stall control for advanced rotorcraft application. *AIAA J*, 1995, **33**, (2), pp 289–295.
3. NAGIB, H., GREENBLATT, D., KIEDAISCH, J., WYGNANSKI, I. and HASSAN, A. Effective flow control for rotorcraft applications at flight Mach number, AIAA paper, 2001-2974, 2001.
4. GLEZER, A. and AMITAY, M. Synthetic jets. *Annual Review of Fluid Mech*, 2003, **34** (34), pp 503–529.
5. REHMAN, A. and KONTIS, K. Synthetic jet control effectiveness on stationary and pitching airfoils, *J Aircr*, 2015, **43** (6), pp 1782–1789.
6. TRAUB, L.W., MILLER, A. and REDINIOTIS, O. Effects of synthetic jet actuation on a ramping NACA 0015 airfoil, *J Aircr*, 2004, **41** (5), pp 1153–1162.
7. HAN, Z.H., ZHANG, K.S., SONG, W.P. and QIAO, Z.D. Optimization of active flow control over an airfoil using a surrogate-management framework, *Aircr*, 2010, **47** (2), pp 603–612.
8. SEIFERT, A., DARABI, A. and WYGNANSKI, I. Delay of airfoil stall by periodic excitation, *AIAA J*, 1999, **33** (4), pp 691–707.
9. SEIFERT, A. and PACK, L.G. Oscillatory excitation of unsteady compressible flows over airfoils at flight Reynolds numbers, AIAA paper, 1999-0925, 1999.
10. GILARRANZ, J.L., TRAUB, L.W. and REDINIOTIS, O.K. Characterization of a compact, high-power synthetic jet actuator for flow separation control, AIAA paper, 2002-0127, 2002.
11. GILARRANZ, J.L., TRAUB, L.W. and REDINIOTIS, O.K. A new class of synthetic jet actuators, Part II: Application to flow separation control, *J Fluids Engineering*, 2005, **127** (2), pp 377–387.
12. LEE, B., KIM, M., LEE, J. and KIM, C. Separation control characteristics of synthetic jets with circular exit array, AIAA paper, 2012-3050, 2012.
13. AMITAY, M., SMITH, D.R. and KIBENS, V.L. Aerodynamic flow control over an unconventional airfoil using synthetic jet actuators, *AIAA J*, 2015, **39** (3), pp 361–370.
14. ZHAO, Q.J., ZHAO, G.Q., WANG, B., WANG, Q., SHI, Y.J. and XU, G.H. Robust Navier-Stokes method for predicting unsteady flowfield and aerodynamic characteristics of helicopter rotor, *Chinese J Aeronautics*, 2018, **31** (2), pp 214–224.
15. ZHAO, Q.J., MA, Y.Y. and ZHAO, G.Q. Parametric analyses on dynamic stall control of rotor airfoil via synthetic jet, *Chinese J Aeronautics*, 2017, **30** (6), pp 1818–1834.

16. SMITH, B.L. and GLEZER, A. The formation and evolution of synthetic jets, *Physics of Fluids*, 1998, **10** (9), pp 2281–2297.
17. DURRANI, D. and HAIDER, B.A., Study of stall delay over a generic airfoil using synthetic jet actuator, AIAA paper, 2011-943, 2011.
18. SANDRA, U. Experimental analysis and analytical modeling of synthetic jet cross flow interactions, Ph.D. Dissertation, University of Maryland, 2007.
19. HASSAN, A.A., STRAUB, F.K. and CHARLES, B.D. Effects of surface blowing/suction on the aerodynamics of helicopter rotor blade-vortex interactions (BVI)- A numerical simulation, *J American Helicopter Society*, 1997, **42** (2), pp 182–194.
20. DINDAR, M., JANSEN, K. and HASSAN, A.A. “Effect of transpiration flow control on hovering rotor blades,” AIAA paper, 1999-3192, 1999.
21. KIM, M., KIM, S., KIM, W., KIM, C. and KIM, Y. Flow control of tiltrotor unmanned-aerial-vehicle airfoils using synthetic jets, *J Aircr*, 2011, **48** (3), pp 1045–1046.
22. ALIMOHAMMADI, S., FANNING, E., PERSOONS, T. and MURRAY, D.B. Characterization of flow vectoring phenomenon in adjacent synthetic jets using CFD and PIV, *Computers & Fluids*, 2016, **140** (25), pp 232–246.
23. KRAL, L.D., DONOVAN, J.F. and CAIN, A.B., “Numerical simulation of synthetic jet actuator,” AIAA paper, 1997-1824, 1997.
24. HE, Y.Y., CARY, A.W. and PETERS, D.A. “Parametric and dynamic modeling for synthetic jet control of a post-stall airfoil,” AIAA paper, 2001-0733, 2001
25. ZHAO, G.Q., ZHAO, Q.J., GU, Y.S. and CHEN, X. Experimental investigations for parametric effects of dual synthetic jets on delaying stall of a thick airfoil, *Chinese J Aeronautics*, 2016, **29** (2), pp 346–357.